INSTITUTE OF PHYSICS PUBLISHING JOURNAL OF MICROMECHANICS AND MICROENGINEERING

J. Micromech. Microeng. **15** (2005) S153–S164 doi:10.1088/0960-1317/15/7/022

MEMS actuators and sensors: observations on their performance and selection for purpose

D J Bell[1,2], T J Lu[1,3], N A Fleck[1] and S M Spearing[4,5]

[1] Department of Engineering, University of Cambridge, UK
[2] Institute of Robotics and Intelligent Systems, ETH Zurich, Switzerland
[3] Department of Engineering Mechanics, Xian Jiaotong University, Xian, People's Republic of China
[4] Department of Aeronautics and Astronautics, Massachusetts Institute of Technology, USA
[5] School of Engineering Sciences, University of Southampton, UK

Received 24 January 2005, in final form 7 April 2005
Published 20 June 2005
Online at stacks.iop.org/JMM/15/S153

Abstract

This paper presents an exercise in comparing the performance of microelectromechanical systems (MEMS) actuators and sensors as a function of operating principle. Data have been obtained from the literature for the mechanical performance characteristics of actuators, force sensors and displacement sensors. On-chip and off-chip actuators and sensors are each sub-grouped into *families*, *classes* and *members* according to their principle of operation. The performance of MEMS sharing common operating principles is compared with each other and with equivalent macroscopic devices. The data are used to construct performance maps showing the capability of existing actuators and sensors in terms of maximum force and displacement capability, resolution and frequency. These can also be used as a preliminary design tool, as shown in a case study on the design of an on-chip tensile test machine for materials in thin-film form.

1. Introduction

The past 25 years have seen microelectromechanical systems (MEMS) transition from being a research curiosity to a multi-billion dollar commercial enterprise. At the same time, the ratio of commercially successful MEMS to the total of prototype devices created as part of research and development efforts is small. In large part this low rate of return is because MEMS development is still in a highly exploratory phase, where all ideas are considered worth exploring. Given the range of MEMS devices that have been attempted it is possible, and timely, to assess the realized performance of devices as a function of operating principle and also to compare with macroscale devices. This exercise is undertaken in the spirit of identifying where opportunities remain to be exploited and also to consolidate our understanding as to what device operating principles are best suited for particular applications. To date the vast majority of MEMS are either sensors or actuators and so it is appropriate to conduct this assessment and comparison for these types of device.

Sensors and actuators are commonly the interface between an engineering system and the physical world. For example, the force or displacement sensors of an electromechanical system convert a mechanical signal into an electrical one; the analog electrical signal from the sensor is then passed to the controller and is amplified, conditioned, converted into digital format, processed, converted back to analog and finally, the electrical signal is converted back into a mechanical signal by a force or displacement actuator. A key contribution of the development of MEMS technology is that it has enabled the integration of sensors, actuators and signal processing on a single chip [1], and their integration has positive effects upon performance, reliability and cost. The ability to integrate actuators on chip leads to the possibility of new distributed control systems [2].

In previous work on the selection of macro actuators [3], performance characteristics have been defined and

Table 1. Families and classes of work mechanical MEMS actuators with force and axial displacement output.

Electrostatic	Piezoelectric	Thermal	Magnetic
Comb drive [38]	Bimorph [39]	Bimorph [40]	Electromagnetic [41]
Scratch drive [42]	Expansion [43]	Solid expansion [44]	Magnetostrictive [45]
Parallel plate [46]		Topology optimized [47]	External field [48]
Inchworm [49]		Shape memory alloy [50]	Magnetic relay [51]
Impact [52]		Fluid expansion [19]	
Distributed [53]		State change [54]	
Repulsive force [55]		Thermal relay [56]	
Curved electrode [57]			
S-shaped [58]			
Electrostatic relay [59]			

presented in graphical form, thus allowing for a systematic comparison of the performance of different categories of actuators. The performance characteristics were estimated from manufacturers' data and from theoretical performance limitations. Subsequently, a database was set up listing relevant attributes of commercial actuators [4]. The database was used to produce performance charts and the practical application of the database was demonstrated in a case study. A similar study has been conducted for commercial macro sensors [5]. To date, no comparable performance charts for MEMS-based actuators and sensors have been developed, and little overall consideration has been given to the relative merits of MEMS actuation and sensing principles [6]. In the existing literature, a wide range of MEMS actuators and sensors has been catalogued but with a focus on fabrication [7]. In previous reviews [8, 9] on MEMS actuators the potential applications of MEMS actuators are described, again with a focus on competing fabrication processes. The application of MEMS technology in automotive sensors and actuators is summarized in [1], but with an emphasis on modelling, design and packaging issues.

This study assesses the performance of MEMS actuators and MEMS force and displacement sensors. Databases of existing MEMS actuators and sensors are created from literature data and these are used to produce performance charts. The charts allow for a comparison of the classes of actuators and sensors, and also allow for a comparison of MEMS and macro actuators in general. The performance charts can also be used as a preliminary design tool, as shown in a case study on the design of an on-chip thin-film tensile test machine. Clearly several other factors, notably issues of manufacturability and reliability, are keys to the ultimate success of an individual device, and these factors must be addressed in the design process; however this lies beyond the scope of the current paper.

2. Classification of MEMS actuators and sensors

There are many different types of MEMS actuator and sensors. In this study, we consider work-producing actuators, force sensors and displacement sensors, fabricated by surface or bulk micromachining.

2.1. MEMS actuators

The *kingdom* of MEMS actuators mainly consists of four *families*: electrostatic, piezoelectric, thermal and magnetic. It is instructive to subdivide each family into *classes*, as shown in table 1. For example, the family of magnetic MEMS actuators comprises the four classes of electromagnetic, magnetostrictive, magnetic relay and external field. The first three of these classes are essentially contained on the chip; however, the external field magnetic actuator has a significant portion of the device mounted off-chip. This indicates a degree of judgement in our methodology. We adopt the pragmatic view that an on-chip device contains most if not all of the operative elements on-chip.

The number of classes is minimized by grouping different actuators together as much as possible. For example, the thermal in-plane flexural actuator [10] is catalogued as a topology-optimized actuator since the geometry is so designed to achieve the required motion through thermal expansion. A representative reference is included in table 1 for each class of actuator, but this is neither exhaustive nor exclusive. Interested readers are directed to [11], which contains the complete database underpinning this work. While on this subject, it is worth noting that published summaries of research on particular devices are often lacking key aspects of the device performance by which it might be compared to other devices. One of the intended contributions of the present paper is to promote more rigorous reporting of device performance data. To this end the classification system presented here can be developed further, with each class sub-divided into a set of *members*, for example, reflecting the many different designs of comb drive which have been demonstrated.

Table 2. Families and classes of MEMS displacement sensors.

Capacitive	AFM	Optical	Electron tunnelling
Parallel plate [60]	Piezoresistive [61]	On chip [62]	[63]
Fringe [64]	Piezoelectric [65]		
	Optical [66]		

2.2. MEMS sensors

The kingdom of MEMS displacement sensors can be structured into the families of capacitive, optical and electron tunnelling, as shown in table 2. In analogous fashion, the kingdom of MEMS force sensors comprises the set of families of piezoresistive, piezoelectric and compliant sensors, as structured in table 3. For the family of compliant force sensors, a displacement sensor is used to measure the deflection of a compliant structure of known stiffness, and this family subdivides into classes of visual and capacitive sensing. For the case of visual sensing, off-chip image capture is by optical

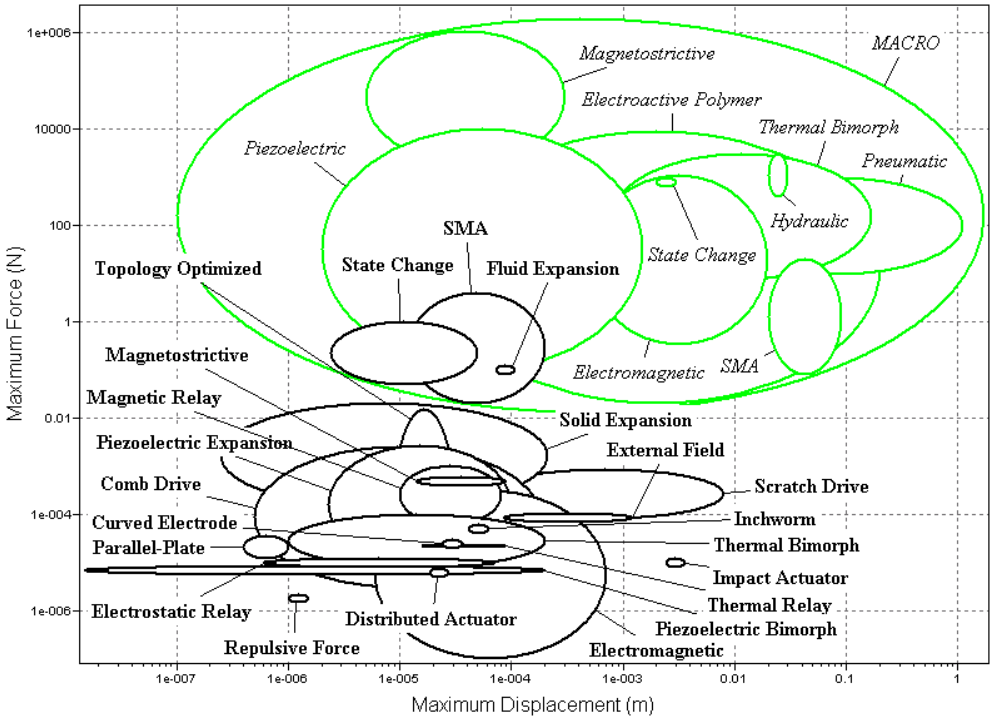

Figure 1. Maximum force versus maximum displacement for MEMS and macro actuators.

Table 3. Families and classes of MEMS force sensors.

Piezoresistive	Piezoelectric	Compliant structure
[67]	[68]	Visual [69] Capacitive [70]

microscopy, confocal optical microscopy, electron microscopy and probe microscopy [12].

2.3. Construction of databases

Databases comprising 120 actuators, 9 displacement sensors and 28 force sensors have been constructed using the software program CES (Cambridge Engineering Selector)[6]. The number of existing truly on-chip displacement sensors is limited, as displacements are usually measured visually off-chip. The actuator database is generated using the performance metrics of maximum force, maximum displacement, displacement resolution and maximum frequency. The displacement sensor database uses the performance characteristics of maximum displacement, displacement resolution and maximum frequency, while the force sensor database uses the performance characteristics of maximum force, force resolution and maximum frequency.

The input data for the three databases were gathered from the existing literature, and came from journal and conference publications on prototype MEMS devices. If, for a certain type of actuator, only one value is found for a characteristic, a range from 80% to 120% of that value is assumed. For cases in which the magnitude of the characteristic is not found, estimates are made using related actuation principles. When no frequency information is reported for an actuator or sensor, the maximum frequency is taken as the natural frequency estimated from a consideration of stiffness and mass.

Alternative performance metrics, such as actuation stress and strain, have been introduced in a previous study [3] on macro actuators but are not used in the current study. It is argued that for MEMS devices the derived quantities of actuation force and displacement are of more practical relevance. It is worth noting, however, that MEMS actuators promise favourable specific stress, work and power due to the trend of enhanced strengths at small scales. These advantages are not realized in the current generation of MEMS actuators due to packaging and integration requirements.

3. Performance charts for MEMS and macro actuators

In this section, performance charts for MEMS and macro-scale actuators and sensors are presented. The charts take as axes performance metrics such as actuator displacement and maximum operating frequency. On each of the performance charts MEMS devices are labelled in bold, and macro devices are labelled in italics. Since the detailed set of macro actuators and sensors have been reviewed elsewhere, only selected macro devices are displayed: the main macro devices are plotted and those with the same operating principle as the MEMS devices are plotted if they exist. The software (CES) used to produce the actuator performance charts plots a given range in the shape of an ellipse. This is somewhat restrictive: a device may possess both the highest maximum force and displacement of its class, and such a device lies (slightly) outside the boundary shown. The performance characteristics of the families of MEMS and macro actuators are summarized in figures 1–3. We consider each figure in turn.

[6] Granta Design Ltd., Unit 300, Rustat House, 62 Clifton Road, Cambridge CB1 7EG, UK.

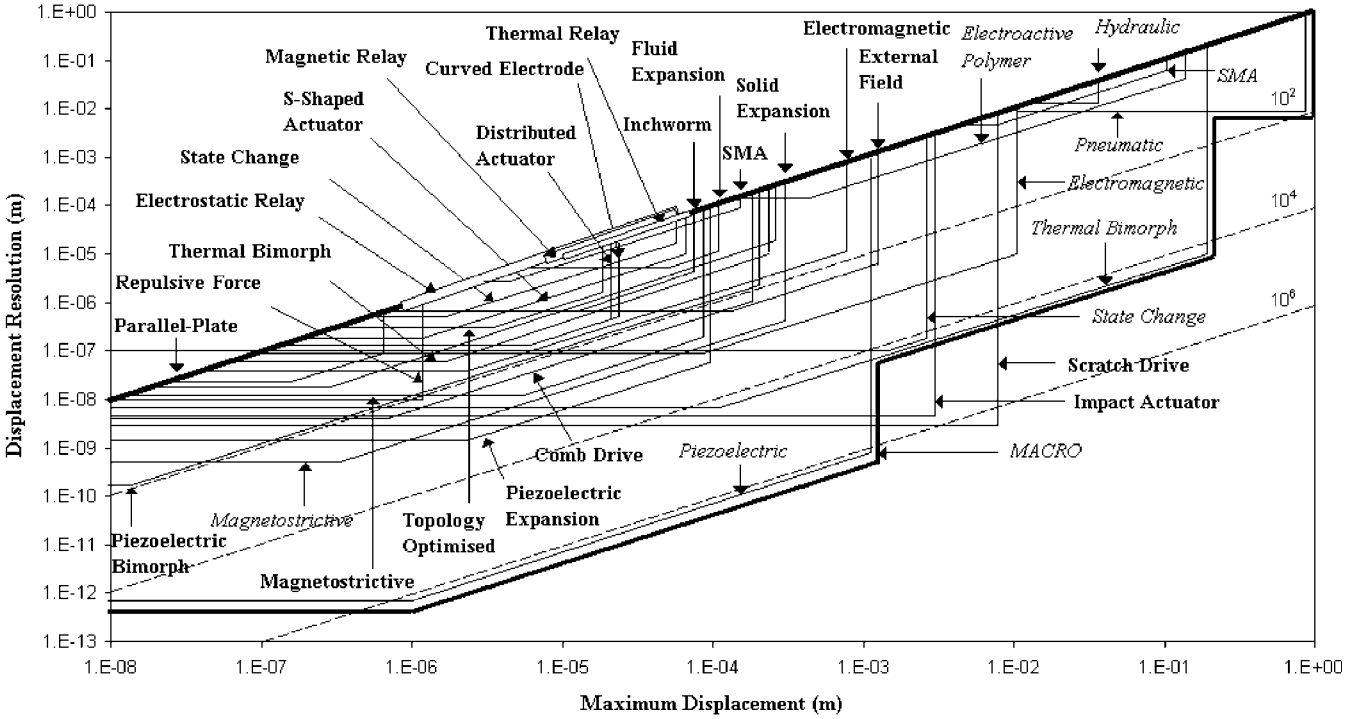

Figure 2. Displacement resolution versus maximum displacement for MEMS and macro actuators.

3.1. Maximum force versus maximum displacement of MEMS and macro actuators

Figure 1 presents a plot of maximum force versus maximum displacement for each class of MEMS actuator, and for macro actuators of the same operating principle taken from Zupan *et al* [4]. The overall envelope of response for the kingdom of macro actuators is also shown. The macro actuators occupy a regime of larger actuation force and displacement than the MEMS actuators, as expected. It is striking from the figure that a larger number of operating principles can be exploited in MEMS actuators than in macro actuators. Many MEMS actuator classes cannot be realized on the macro scale. This is partly due to the differences in manufacturing routes and partly due to the nature of the scaling laws of the underlying physics. For example, the MEMS-based electrostatic comb drive has a narrow gap between the electrodes and can thereby produce a high electric field; since this gap is less than the mean free path of air molecules, the breakdown electric field is high and a satisfactory performance can be achieved [13]. At larger length scales the performance deteriorates, and hence the macro equivalent of the comb drive does not exist. However, the reverse is also true for certain types of macro actuators. Some macro actuator classes do not have an equivalent MEMS actuator class. This can be due to the difficulty in manufacturing to tight tolerances and to excessive wear rates with diminishing scale, as in the case of pneumatic and hydraulic actuators. There remains an opportunity to downsize macro actuators to the MEMS level.

3.1.1. Characteristics of MEMS actuators. Upon comparing the different MEMS families, it is noted that the most ubiquitous family, electrostatic actuators, have a force output lying mid-range at 10^{-6} N–10^{-3} N, but can offer relatively large displacements of up to 200 μm. This can be further enhanced by the use of repeated motions or ratchetting mechanisms, as in scratch drives and impact actuators. The displacement output of scratch drives and impact actuators is only limited by the size of the substrate. The highest forces [14] and the highest displacements [15] of comb drives are achieved by using topology optimized designs.

The force output of both electromagnetic and magnetostrictive actuators is relatively low. Forces induced by magnetic fields scale disadvantageously into the microscale [16]. Typically, the maximum achievable force is between 10^{-7} N and 10^{-4} N, and the maximum displacement is between 10^{-5} m and 10^{-3} m. To raise the work output of microscale devices, materials with higher magnetic energy density are required. Current material choices for micromagnets are not optimal for magnetic performance, as the choice is limited to those materials that can be micromachined.

The maximum force of piezoelectric actuators is typically between 10^{-5} and 10^{-3} N and the maximum displacement between 10^{-7} and 10^{-3} m. Due to the existence of a range of viable piezoelectric materials, a broad set of design specifications can be met. Three groups of materials have been used: low strain piezoelectrics can strain by up to about 3×10^{-5}, high strain piezoelectrics can strain by up to about 2×10^{-4} and piezoelectric polymers can strain by up to 1×10^{-3} [3]. Since a higher piezoelectric strain coefficient implies a lower Young's modulus, the selection of material for a piezoelectric actuator is a trade-off between force and displacement. One class of piezoelectric actuators is the piezoelectric bimorph, which exhibits larger displacement output at the expense of lower force output. MEMS piezoelectric actuators do not significantly exceed the performance of MEMS electrostatic actuators. This reflects the limitations in the available materials and in the achievable geometries.

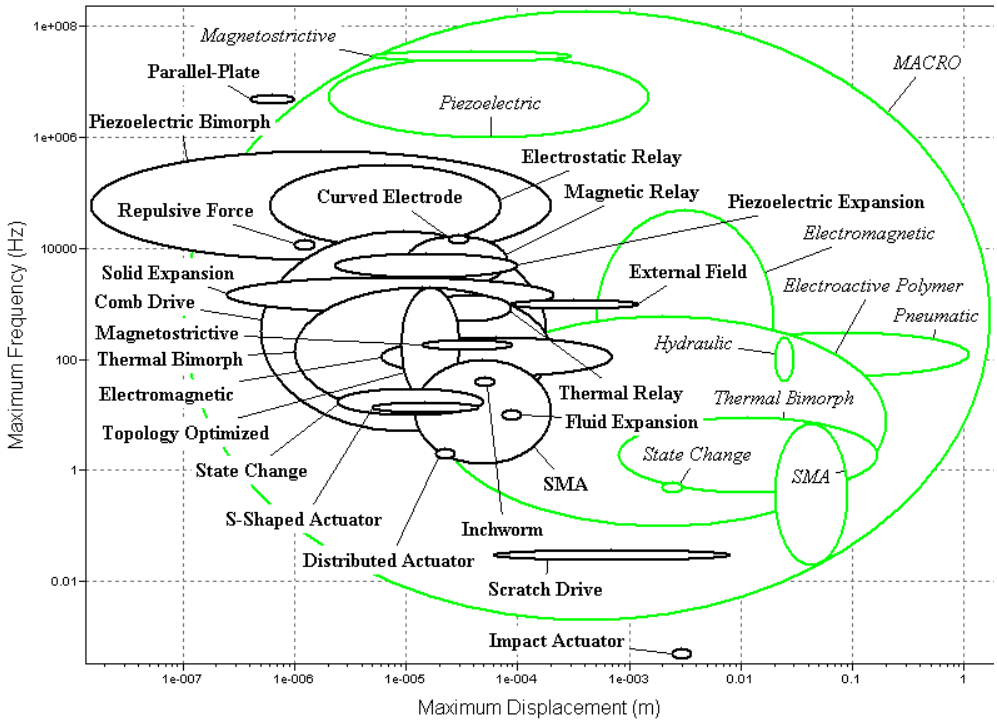

Figure 3. Maximum frequency versus maximum displacement for MEMS and macro actuators.

MEMS actuators with the highest force capability rely upon temperature excursions for their operation: shape memory alloy (SMA) actuators, state change actuators, solid expansion and fluid expansion actuators. The SMA actuators offer the highest force capacity along with a moderate displacement. Large strains of up to 10% and stresses of up to 500 MPa are possible [17, 18]. The performance of SMA actuators can be further improved by using topology optimized designs, like the flexural actuator comprising a triangular corrugated core with SMA faces considered by Lu *et al* [19]. Actuators based on a state change or fluid expansion also provide high energy densities, resulting in a high force and displacement output. It has been shown that the use of a corrugated diaphragm increases the deflection range significantly for these types of actuators [20]. Thermal expansion actuators can deliver a wide spectrum of displacements and forces depending upon the choice of expansion materials. For large actuation displacement, the thermal expansion coefficient is maximized, typically requiring the use of polymers [3]. Thermal bimorph actuators offer a high displacement output at the expense of a lower force output both on-chip and off-chip.

3.2. Displacement resolution versus maximum displacement of MEMS and macro actuators

In figure 2, the displacement resolution is plotted against the maximum displacement for MEMS actuators and a variety of commercial macro actuators, as reviewed by Zupan *et al* [4]. The bold line of slope +1 defines the limit where the resolution is equal to the maximum displacement. The three classes of relays lie on this boundary. The further away from this boundary an actuator lies the more actuation positions are achievable. In general MEMS actuators offer better resolution than macro-scale devices, although the best resolution of all actuator classes is provided by macro-scale piezoelectric devices. In part this is a result of using stacked actuators with individually addressable layers, a geometry that has not yet been realized in MEMS.

In comparison with macro actuators, the resolution of MEMS actuators relative to their maximum displacement is limited; most of them have less than 10^3 discrete positions, with a clustering along the line for a single bit performance, where the resolution equals the range. The envelope of MEMS actuators is within the envelope of macro actuators, in contrast to figure 1.

3.3. Maximum frequency versus maximum displacement of MEMS and macro actuators

Figure 3 contains a plot of maximum frequency versus maximum displacement for each class of MEMS actuator and a variety of commercial macro actuators [4]. It is striking that MEMS actuators exist over a frequency range from 1 Hz to about 10^5 Hz for a maximum displacement of 1–100 μm.

The macro actuators with the highest frequency response ($\sim 10^7$ Hz) are based upon active materials such as those with magnetostrictive and piezoelectric responses. In contrast, the MEMS versions of these actuators have a relatively poor frequency response. The MEMS devices usually contain thin films operating in bending or are integrated with a lever, and both approaches result in low natural frequencies. For all actuator families apart from the thermal actuators, the maximum frequency is limited by the first resonant frequency. The frequency capability of thermal actuators is limited by the time required to transfer heat into and out of the actuator. The heat transfer depends on convection at the surface of the actuator [3] and its specific heat capacity and dimensions. Only the frequency performance of the family of thermal MEMS actuators exceeds that of their equivalent

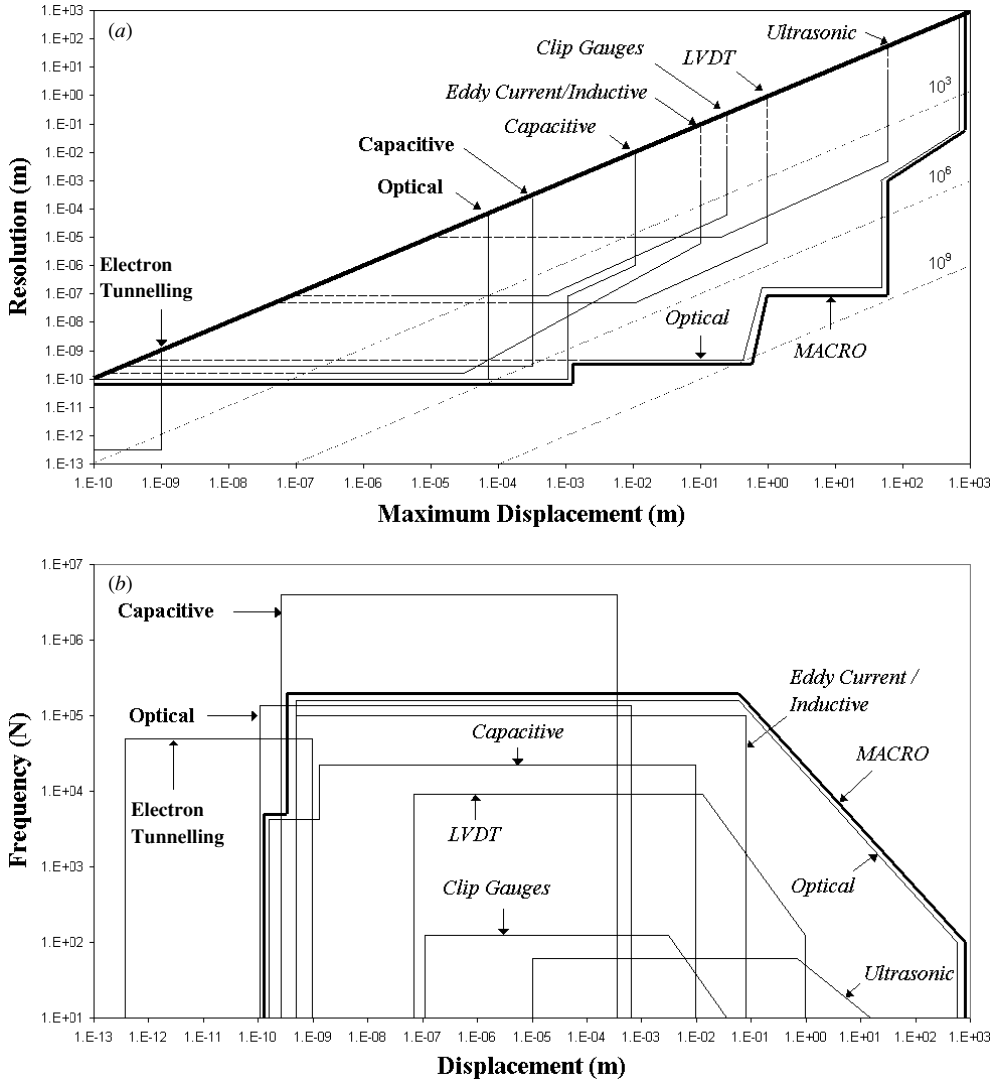

Figure 4. (*a*) Displacement resolution versus maximum displacement and (*b*) frequency versus displacement for MEMS and macro displacement sensors.

macro actuators, which is illustrated by the difference between MEMS and macro SMA actuators, state change actuators and thermal bimorphs in figure 3. The frequency capability of MEMS thermal actuators is comparable to other actuation principles due to the faster heat removal capability at the micro-scale, which is caused by the increase in the ratio of surface to volume. In contrast, the frequency of macro thermal actuators (e.g. SMA, state change actuators and thermal bimorphs) is less than 10 Hz.

4. Performance charts for MEMS and macro sensors

4.1. Maximum displacement, resolution and maximum frequency of MEMS and off-chip macro sensors for displacement

Figure 4(*a*) contains a plot of resolution versus maximum displacement, while figure 4(*b*) gives the maximum frequency versus displacement for both MEMS displacement sensors and commercial macro displacement sensors as compiled by Shieh *et al* [5]. Again, for the sake of clarity, only the main macro sensors are shown, including those which share the same operating principle as the MEMS sensors; see [5] for a full plot of the performance characteristics of macro sensors. The abscissa labelled 'displacement' shown in figure 4(*b*) defines the operating regime for the displacement sensors: the lower limit for each class of device is the minimum resolution while the upper limit equals the maximum displacement achievable. Similarly, the ordinate of figure 4(*b*) labelled 'frequency' denotes the operational frequency.

The plot of resolution versus maximum displacement, figure 4(*a*), contains a set of parallel lines of slope +1, denoting the number of discrete displacement values, which can be measured in an analog to digital conversion. The uppermost bold line defines the limiting case where the resolution equals the range; on/off switches are of this type.

The MEMS displacement sensors can measure much smaller maximum displacements than macro displacement sensors. Also their resolution is less: MEMS displacement sensors have a ratio of maximum displacement to resolution of at most 10^6, whereas off-chip macro sensors can attain a ratio of up to 10^9. This difference is partly due to different operating principles, and partly because it is difficult to manufacture MEMS devices to a tight tolerance. The MEMS-based electron tunnelling sensors have a resolution of down to 10^{-12} m and

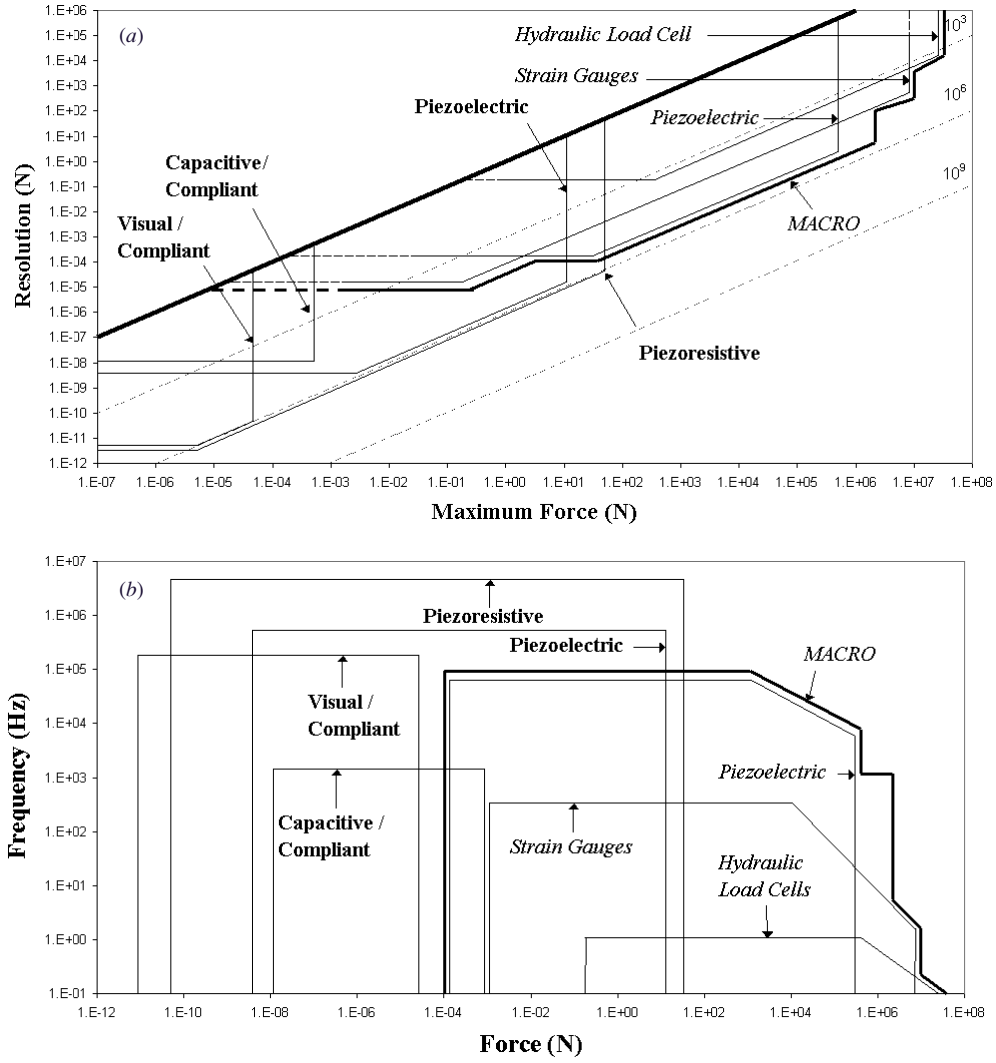

Figure 5. (*a*) Force resolution versus maximum force and (*b*) frequency versus force for MEMS and macro force sensors.

a maximum displacement capability of about 1 nm, because tunnelling can only occur over that distance.

MEMS displacement sensors typically have a higher maximum frequency capability than off-chip devices, and can detect displacements of up to 10^7 Hz (figure 4(*b*)). The maximum frequency can be limited by various factors. For some devices such as capacitive sensors, the frequency is limited by the natural frequency of the structure; for others, such as optical displacement sensors, it is limited by electronic and environmental noise. Capacitive MEMS displacement sensors exhibit improved frequency performance compared to macro sensors, since the natural frequency of the sensing structure increases with decreasing mass.

4.2. Maximum force, resolution and maximum frequency of MEMS and off-chip macro sensors for force

Figure 5(*a*) contains a plot of force resolution versus maximum force, while figure 5(*b*) gives the frequency versus force for both MEMS force sensors and commercial macro sensors as compiled by Shieh *et al* [5]. Again, for the sake of clarity, only the main macro sensors are shown, including those which share the same operating principle as the MEMS sensors; see [20] for a full plot of the performance characteristics of macro sensors. The plot in figure 5(*b*) gives the achievable forces for each class of device: the lower limit of the envelope for each class is the force resolution while the upper limit is the maximum achievable force.

It is evident from figures 5(*a*) and (*b*) that MEMS force sensors exhibit better resolution than macro sensors but at the expense of a lower maximum force capability. The achievable resolution for MEMS force sensors goes down to 10^{-11} N, while the maximum measurable force is approximately 10 N. For macro force sensors, the best achievable resolution is 10^{-5} N and the maximum force is 10^7 N. Piezoresistive MEMS force sensors offer the best force sensor performance in terms of resolution, range and frequency. Piezoelectric sensors have comparable resolution and frequency capability. However, they are not capable of measuring a static force due to the leakage of electrostatic charge [20]. The resolution of visual/compliant force sensors can be better than the resolution of capacitive/compliant sensors, but at the expense of a much more compliant device. The visual/compliant force sensor can make use of a highly compliant cantilever beam which deflects under load. The resolution of visual/compliant force sensors can also be improved significantly by correlating displacements with changes in light intensity [21]. Force sensors based on a compliant structure also exist on the macro scale. They usually employ strain gauges and are labelled

Table 4. Existing MEMS mechanical test machines.

Machine	Actuator	Force sensor	Displacement sensor	References
1	Comb drive	–	Capacitive	[27]
2	Comb drive	–	Optical (off-chip)	[28]
3	Solid expansion	–	Optical (off-chip)	[29]
4	Comb drive	Visual/compliant	Optical (off-chip)	[30]
5	Parallel-plate	–	Optical (off-chip)	[32]
6	Comb drive	–	Optical (off-chip)	[31]

Table 5. Parameters of interest for preliminary design of on-chip tensile test machine.

Maximum force	1 mN
Maximum actuator displacement	10 μm
Actuator displacement resolution	10 nm
Maximum displacement sensor displacement	1 μm
Displacement sensor resolution	1 nm
Force sensor resolution	1 μN

'strain gauges' in figures 5(*a*) and (*b*). Commercial load cells are of this type.

5. Case study: design of on-chip tensile test machine

By way of an example of how the results of the previous sections might be applied to a practical problem, the results have been applied to examine the selection of sensors and actuators for a micromechanical test device. This is motivated by the fact that many commercial MEMS devices are made from thin films. In order to design devices with sufficient reliability, the mechanical properties of the thin films need to be known. The mechanical properties of a thin-film material cannot be assumed to be the same as those of bulk material [13, 23], as the thin film may have a non-equilibrium microstructure and the film thickness can interact with the characteristic length scale of the deformation mechanism. Consequently, tests have to be carried out on specimens of similar size to those used in a MEMS structure [13]. Although a number of microscale mechanical test methods have been developed [23], it is unclear whether it is feasible to develop an on-chip mechanical test machine in order to probe the properties of thin films or whether it is worth developing in comparison with an off-chip test machine.

Typical examples of techniques hitherto employed for this task are indentation tests [24], bending tests [25] and resonance tests [26]. The uniaxial tensile test remains the preferred choice to obtain the most accurate, unambiguous data for both elastic and plastic properties of the material. However, in order to perform a successful tensile test the following practical considerations need to be addressed: (i) handling and gripping of the specimen, and alignment with the direction of the applied force, (ii) the generation and measurement of small forces and displacements and (iii) accounting for the effects of friction and machine compliance. One way to meet these challenges is to integrate the test machine on a single chip. Existing on-chip test machines are now reviewed.

Van Arsdell and Brown [27] and Kahn *et al* [28] initiated crack propagation in polysilicon in bending with a comb drive actuator. Kapels *et al* [29] used thermal actuation to study fracture strength and fatigue of polysilicon in tension. Dai [30] carried out on-chip bending tests to measure Young's modulus of thin films. Jeong *et al* [31] performed resonance tests with a comb drive actuator to evaluate the elastic properties of single-crystalline silicon. Only Haque and Saif [32] have used a truly on-chip tensile test machine to measure thin-film properties. Their machine uses a comb drive actuator, a force sensor in the form of a buckling beam and an off-chip optical microscope to measure the displacement of an on-chip Vernier gauge. The types of actuator, force sensor and displacement sensor used in these on-chip test machines are summarized in table 4.

The typical requirements for a thin-film tensile test machine are listed in table 5. Any conceptual design involves the selection of an appropriate actuator, displacement sensor and force sensor; this task is now performed by making use of the data plotted in figures 1–5.

Table 6. Check for preliminary design requirements.

Class	Maximum force	Maximum displacement	Resolution
Actuator			
Comb drive	Yes	Yes	Yes
Scratch drive	Yes	Yes	Yes
Parallel plate	No	No	Yes
Inchworm	No	Yes	No
Impact	No	Yes	No
Distributed	No	Yes	Yes
Repulsive force	No	No	Yes
Curved electrode	No	Yes	No
S-shaped	No	Yes	No
Electrostatic relay	No	Yes	No
Piezoelectric bimorph	No	Yes	Yes
Piezoelectric expansion	Yes	Yes	Yes
Thermal bimorph	No	Yes	No
Solid expansion	Yes	Yes	Yes
Topology optimized	Yes	Yes	No
Shape memory alloy	Yes	Yes	No
Fluid expansion	Yes	Yes	No
State change	Yes	Yes	No
Thermal relay	No	Yes	No
Electromagnetic	No	Yes	Yes
Magnetostrictive	No	Yes	Yes
External field	No	Yes	No
Magnetic relay	Yes	Yes	No
Displacement sensor			
Capacitive	–	Yes	Yes
Piezoresistive	–	Yes	Yes
Piezoelectric	–	Yes	Yes
Electron Tunnelling	–	No	Yes
Optical	–	Yes	Yes
Force sensor			
Piezoresistive	Yes	–	Yes
Piezoelectric	Yes	–	Yes
Visual/compliant	No	–	Yes
Capacitive/compliant	Yes	–	Yes

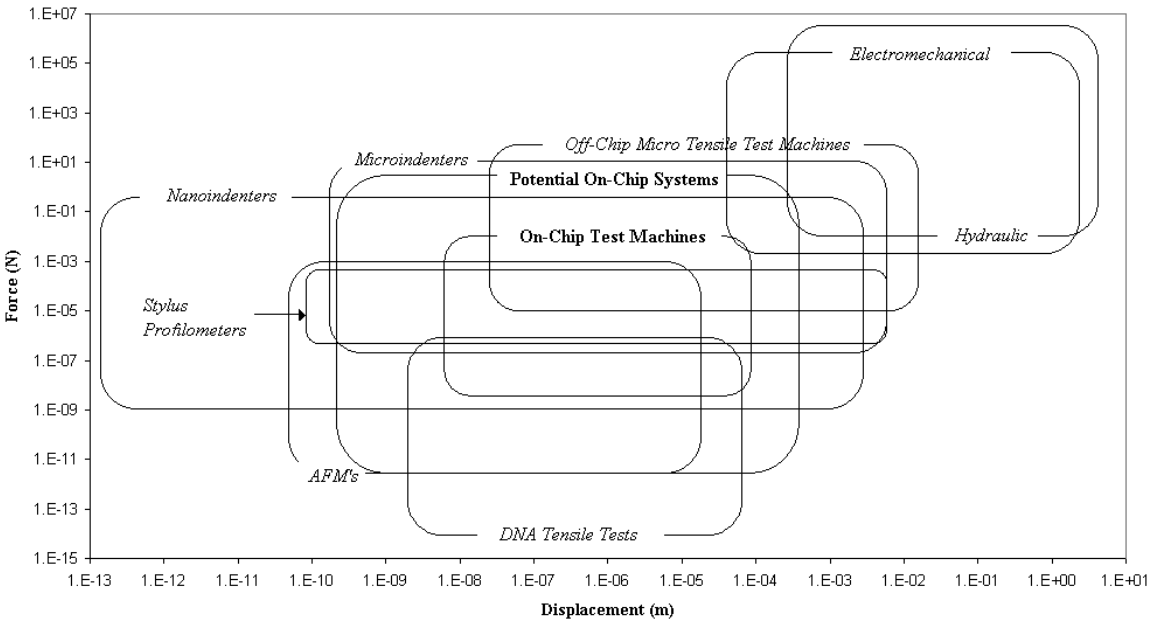

Figure 6. Force versus displacement for on-chip MEMS and macro mechanical test machines.

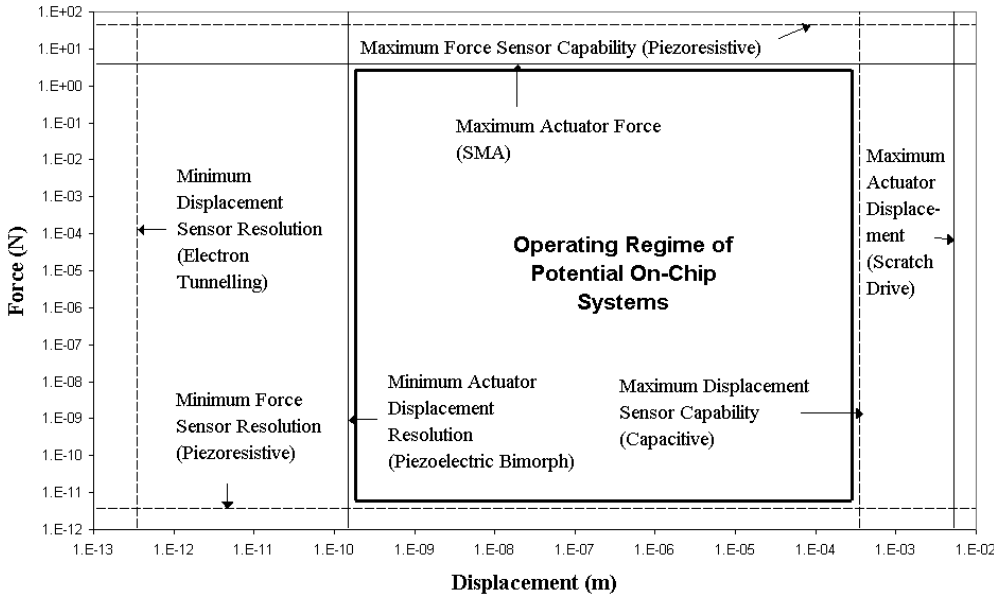

Figure 7. Operating regime of potential on-chip systems.

First, only a sub-set of the actuators reviewed in figure 1 possess the required force and displacement capabilities: comb drive, scratch drive, piezoelectric expansion, thermal solid expansion, topology optimized, SMA, fluid expansion, state change and magnetic relay. A consideration of the displacement resolution shown in figure 2 narrows the list further to the comb drive, scratch drive, piezoelectric expansion and thermal solid expansion. A final choice can only be made by consideration of manufacturability and costs, and is considered no further here. Second, we select an appropriate displacement sensor. Figure 4 suggests that capacitive and optical sensors are candidates. A non-contact technique is preferred for displacement sensing. The interferometry technique of Sharpe *et al* [33], and improved subsequently by Zupan and Hemker [34], is the best choice. Third, an appropriate force sensor is selected. Figure 5 identifies piezoresistive, piezoelectric and capacitive/compliant force sensors as having the necessary force capability and resolution. Table 6 summarizes the candidate actuators and sensors, which meet the preliminary design requirements. It is concluded that an on-chip tensile test machine for thin-film materials is feasible, and suitable sensors and actuators have been identified.

6. A comparison of on-chip and off-chip test machines

It is instructive to compare the performance of existing MEMS mechanical test machines with off-chip macro machines such as the servo-hydraulic test machine. Additionally, *potential on-chip systems* can be conceptually designed from new

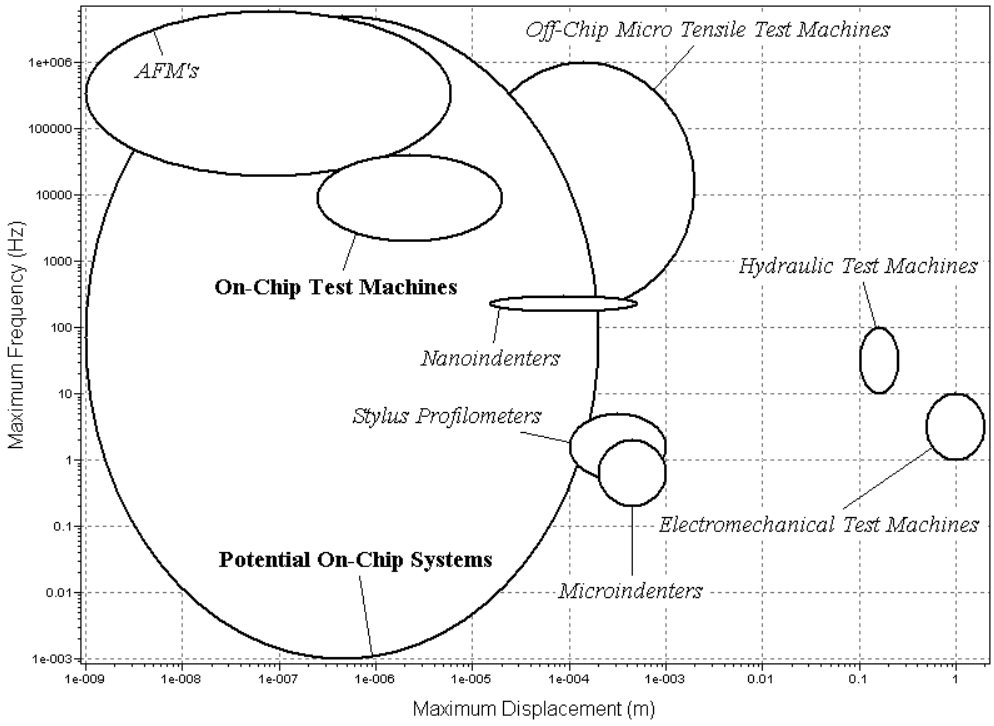

Figure 8. Maximum frequency versus maximum displacement for on-chip MEMS and macro mechanical test machines.

combinations of actuator, displacement sensor and force sensor and the combined performance can be predicted.

6.1. Force versus displacement of mechanical test machines

The force versus displacement capacity is plotted in figure 6 for various mechanical test machines including on-chip test machines. As before, the minimum force shown by each envelope denotes the resolution, while the maximum force is given by the upper limit; the displacement parameter given in the abscissa has a similar interpretation.

The operating envelope for on-chip MEMS test machines comes from the published set of machines, as described in the previous section. The envelope for potential on-chip systems contains the intersection set of all viable combinations of MEMS actuators, displacement sensors and force sensors (figure 7). The data for each class of macro test machine come from the websites of various manufacturers and from the published literature. The force in figure 6 spans 21 orders of magnitude while the displacement spans 13 orders of magnitude. Potential on-chip systems cover a significant proportion of the full range. In contrast, the existing set of on-chip test machines have a performance which is mid-range compared to off-chip machines. A similar performance can be achieved by macroscale or hybrid approaches such as modified AFMs or nanoindenters. Indeed, a reconfigured nanoindenter has been used to carry out thin-film tensile tests [35, 36].

Low force levels in DNA tensile tests are typically achieved by using optical tweezers [37]. The magnitude of displacement measured in biological specimens is comparable to that measured by other test systems. In AFMs low force levels are achieved through the combination of high displacement resolution macro piezoelectric actuator and high force resolution beam sensor.

6.2. Maximum frequency versus maximum displacement of mechanical test machines

Dynamic testing in creep and fatigue are important mechanical tests, and so it is helpful to plot in figure 8 the maximum frequency and maximum displacement capabilities of the same test machines given in figure 6. The maximum frequency for potential on-chip systems is limited by the capability of MEMS actuators: a wide range of frequency capabilities is anticipated due to the large spread in frequency performance of MEMS actuators. The AFM exhibits an exceptionally high frequency response due to the small size of its cantilever beam.

7. Concluding remarks

The present study presents a comparison of the mechanical performance of MEMS-based actuators, displacement sensors and force sensors. Both MEMS actuators and sensors are compared to macro actuators and sensors. Performance maps show the capability of existing MEMS (and macro) actuators and sensors in terms of maximum force and displacement capability, resolution and frequency. They can be used as a preliminary design tool, as shown in the case study on the design of an on-chip thin-film tensile test machine.

MEMS actuators generally occupy a distinct part of the force versus displacement performance chart.

The performance of MEMS sensors is superior to macro sensors in terms of resolution and maximum frequency. This explains why a variety of commercial MEMS sensors, such as accelerometers and pressure sensors, are widely used. The low manufacturing costs and small package size also play a major role in the success of these devices.

Existing on-chip test machines do not offer a unique capability in terms of force and displacement. Similar performances can be achieved by macroscale or hybrid

approaches such as modified AFMs or nanoindenters. However, there remains much scope for developing new MEMS-based on-chip test machines. By careful selection of actuator and sensors, a wide regime of force and displacement capacity is anticipated with a wideband frequency response.

Finally, our overarching hope in presenting this work is that it will prompt more rigorous assessment and presentation of experimental data for the performance of MEMS. We believe that this will become increasingly important as the field matures and funding for research activities becomes less available. The performance assessment and selection methodology presented herein may provide a useful framework for comparing such data.

Acknowledgments

The authors would like to thank the Cambridge-MIT Institute (CMI) for funding this work. SMS holds a Royal Society Wolfson Research Merit Award. TJL would also like to thank the National Science Foundation of China (grant no. 10328203) for partial financial support.

References

[1] Eddy D S and Sparks D R 1998 Application of MEMS technology in automotive sensors and actuators *Proc. IEEE* **86** 1747–55

[2] Frank R 2000 *Understanding Smart Sensors* (Boston, MA: Artech House)

[3] Huber J E, Fleck N A and Ashby M F 1997 The selection of mechanical actuators based on performance indices *Proc. R. Soc.* A **453** 2185–205

[4] Zupan M, Ashby M F and Fleck N A 2002 Actuator classification and selection—the development of a database *Adv. Eng. Mater.* **4** 933–9

[5] Shieh J, Huber J E, Fleck N A and Ashby M F 2001 The selection of sensors *Prog. Mater. Sci.* **46** 461–504

[6] Srikar V T and Spearing S M 2003 Materials selection for microfabricated electrostatic actuators *Sensors Actuators* A **102** 279–85

[7] Kovacs G T A 1999 *Micromachined Transducers Sourcebook* (New York: McGraw-Hill)

[8] Thielicke E and Obermeier E 2000 Microactuators and their technologies *Mechatronics* **10** 431–55

[9] Fujita H 1998 Microactuators and micromachines *Proc. IEEE* **86** 1721–32

[10] Hickey R, Sameoto D, Hubbard T and Kujath M 2003 Time and frequency response of two-arm micromachined thermal actuators *J. Micromech. Microeng.* **13** 40–6

[11] Bell D J 2003 The development of a tensile test machine for MEMS *MPhil. Thesis* Cambridge University Engineering Department

[12] Wang X 2002 Vision-based characterization, manipulation, and control of objects using compliant tools *PhD Dissertation* Philadelphia

[13] Spearing S M 2000 Materials issues in MEMS *Acta Mater.* **48** 179–96

[14] Rodgers M S, Kota S, Hetrick J, Li Z, Jensen B D, Krygowski T W, Miller S L, Barnes S M and Burg M S 2000 A new class of high force, low-voltage, compliant actuation systems *Solid-State Sensor and Actuator Workshop (Hilton Head Island, SC)*

[15] Grade J D, Jerman H and Kenny T W 2003 Design of large deflection electrostatic actuators *J. Microelectromech. Syst.* **12** 335–43

[16] Madou M 1997 *Fundamentals of Microfabrication* (Boca Raton, FL: CRC)

[17] Krulevitch P, Lee A P, Ramsey P B, Trevino J C, Hamilton J and Northrup M A 1996 Thin film shape memory alloy microactuators *J. Microelectromech. Syst.* **5** 270–81

[18] Srinivasan A V and McFarland D M 2000 *Smart Structures* (Cambridge: Cambridge University Press)

[19] Lu T J, Hutchinson J W and Evans A G 2001 Optimal design of a flexural actuator *J. Mech. Phys. Solids* **49** 2071–93

[20] Jeong O C and Yang S S 2000 Fabrication of a thermopneumatic microactuator with a corrugated p+ silicon diaphragm *Sensors Actuators* **80** 62–7

[21] Davis C Q and Freeman D M 1998 Statistics of subpixel registration algorithms based on spatiotemporal gradients or block matching *Opt. Eng.* **37** 1290–8

[22] Vinci R P and Vlassak J J 1996 Mechanical behavior of thin films *Annu. Rev. Mater. Sci.* **26** 431–62

[23] Srikar V T and Spearing S M 2003 A critical review of microscale mechanical testing methods used in the design of microelectromechanical systems (MEMS) *Exp. Mech.* **43** 228–37

[24] Stone D S 1989 Indentation technique to investigate elastic moduli of thin films on substrate *Thin Films: Stress and Mechanical Properties* vol 130 (Pittsburgh, PA: Materials Research Soc.) pp 105–10

[25] Johansson S, Schweitz J-A, Tenerz L and Tiren J 1988 Fracture testing of silicon microelements *in situ* in a scanning electron microscope *J. Appl. Phys.* **63** 4799–803

[26] Petersen K E and Guarnieri C R 1979 Young's modulus measurements of thin films using micromechanics *J. Appl. Phys.* **50** 6761–6

[27] Van Arsdell W W and Brown S B 1999 Subcritical crack growth in silicon MEMS *J. Microelectromech. Syst.* **8** 319–27

[28] Kahn H, Tayebi N, Ballarini R, Mullen R L and Heuer A H 1999 Fracture and fatigue of polysilicon MEMS devices *Transducers '99 (Sendai)*

[29] Kapels H, Aigner R and Binder J 2000 Fracture strength and fatigue of polysilicon determined by a novel thermal actuator *IEEE Trans. Electron Devices* **47** 1522–8

[30] Dai C-H 2003 *In situ* electrostatic microactuators for measuring the Young's modulus of CMOS thin films *J. Micromech. Microeng.* **13** 563–7

[31] Jeong J-H, Chung S-H, Lee S-H and Kwon D 2003 Evaluation of elastic properties and temperature effects in Si thin films using an electrostatic microresonator *J. Microelectromech. Syst.* **12** 524–30

[32] Haque M A and Saif M T A 2001 Microscale materials testing using MEMS actuators *J. Microelectromech. Syst.* **10** 146–52

[33] Sharpe W N Jr, Yuan B and Edwards R L 1997 A new technique for measuring the mechanical properties of thin films *J. Microelectromech. Syst.* **6** 193–9

[34] Zupan M and Hemker K J 2002 Application of Fourier analysis to the laser based interferometric strain/displacement gage *Exp. Mech.* **42** 214–20

[35] LaVan D A and Buchheit T E 2000 Testing of critical features of polysilicon MEMS *Mater. Res. Soc. Symp. Proc.* **605** 19–24

[36] LaVan D A, Hohlfelder R J, Sullivan J P, Friedmann T A, Mitchell M and Ashby C I H 2000 Tensile properties of amorphous diamond films *Mater. Res. Soc. Symp. Proc.* **594** 295–300

[37] Bao G 2002 Mechanics of biomolecules *J. Mech. Phys. Solids* **50** 2237–74

[38] Zhao Y and Cui T 2003 Fabrication of high-aspect-ratio polymer-based electrostatic comb drives using the hot embossing technique *J. Micromech. Microeng.* **13** 430–5

[39] Zhang Q Q, Gross S J, Tadigadapa S, Jackson T N, Djuth F T and Trolier-McKinstry S 2003 Lead zirconate titanate films for d33 mode cantilever actuators *Sensors Actuators* A **105** 91–7

[40] Sehr H, Tomlin I S, Huang B, Beeby S P, Evans A G R, Brunnschweiler A, Ensell G J, Schabmueller C G J and

Niblock T E G 2002 Time constant and lateral resonances of thermal vertical bimorph actuators *J. Micromech. Microeng.* **12** 410–3
[41] Cho H J and Ahn C H 2002 A bidirectional magnetic microactuator using electroplated permanent magnet arrays *J. Microelectromech. Syst.* **11** 78–84
[42] Li L, Brown J G and Uttamchandani D 2002 Study of scratch drive actuator force characteristics *J. Micromech. Microeng.* **12** 736–41
[43] Koganezawa S, Uematsu Y, Yamada T, Nakano H, Inoue J and Suzuki T 1999 Dual-stage actuator system for magnetic disk drives using a shear mode piezoelectric microactuator *IEEE Trans. Magn.* **35** 988–92
[44] Butler J T, Bright V M and Cowan W D 1999 Average power control and positioning of polysilicon thermal actuators *Sensors Actuators* **72** 88–97
[45] Bourouina T, Lebrasseur E, Reyne G, Debray A, Fujita H, Ludwig A, Quandt E, Muro H, Oki T and Asaoko A 2002 Integration of two degree-of-freedom magnetostrictive actuation and piezoresistive detection: application to a two-dimensional optical scanner *J. Microelectromech. Syst.* **11** 355–60
[46] Yao J J, Arney S C and MacDonald N C 1992 Fabrication of high frequency two-dimensional nanoactuators for scanned probe devices *J. Microelectromech. Syst.* **1** 14–22
[47] Moulton T and Ananthasuresh G K 2001 Micromechanical devices with embedded electro-thermal-compliant actuation *Sensors Actuators* A **90** 38–48
[48] Khoo M and Liu C 2001 Micro magnetic silicone elastomer membrane actuator *Sensors Actuators* A **89** 259–66
[49] Yeh R, Hollar S and Pister K S J 2002 Single mask, large force, and large displacement electrostatic linear inchworm motors *J. Microelectromech. Syst.* **11** 330–5
[50] Roch I, Bidaud P, Collard D and Buchaillot L 2003 Fabrication and characterization of an SU-8 gripper actuated by a shape memory alloy thin film *J. Micromech. Microeng.* **13** 330–6
[51] Ruan M, Shen J and Wheeler C B 2001 Latching micromagnetic relays *J. Microelectromech. Syst.* **10** 511–7
[52] Mita M, Arai M, Tensaka S, Kobayashi D and Fujita H 2003 A micromachined impact microactuator driven by electrostatic force *J. Microelectromech. Syst.* **12** 37–41
[53] Minami K, Kawamura S and Esashi M 1993 Fabrication of distributed electrostatic micro actuator (DEMA) *J. Microelectromech. Syst.* **2** 121–7
[54] Carlen E T and Mastrangelo C H 2002 Electrothermally activated paraffin microactuators *J. Microelectromech. Syst.* **11** 165–73
[55] Lee K B and Cho Y 2001 Laterally driven electrostatic repulsive-force microactuators using asymmetric field distribution *J. Microelectromech. Syst.* **10** 128–36
[56] Gomm T, Howell L L and Selfridge R H 2002 In-plane linear displacement bistable microrelay *J. Micromech. Microeng.* **12** 257–64
[57] Legtenberg R, Gilbert J, Senturia S D and Elwenspoek M 1997 Electrostatic curved electrode actuators *J. Microelectromech. Syst.* **6** 257–65
[58] Shikida M, Sato K and Harada T 1997 Fabrication of an S-shaped microactuator *J. Microelectromech. Syst.* **6** 18–24
[59] Lee H-S, Leung C H, Shi J, Chang S-C, Lorincz S and Nedelescu I 2002 Integrated microrelays: concept and initial results *J. Microelectromech. Syst.* **11** 147–53
[60] Chu L L and Gianchandani Y B 2003 A micromachined 2D positioner with electrothermal actuation and sub-nanometer capacitive sensing *J. Micromech. Microeng.* **13** 279–85
[61] Brook A J, Bending S J, Pinto J, Oral A, Ritchie D, Beere H, Springthorpe A and Henini M 2003 Micromachined III–V cantilevers for AFM-tracking scanning Hall probe microscopy *J. Micromech. Microeng.* **13** 124–8
[62] Haronian D 1998 In-plane degree of freedom optical waveguide displacement sensors based on geometrical modulation *Sensors Actuators* **69** 217–25
[63] Kenny T W, Kaiser W J, Rockstad H K, Reynolds J K, Podosek J A and Vote E C 1994 Wide-bandwidth electromechanical actuators for tunneling displacement transducers *J. Microelectromech. Syst.* **3** 97–103
[64] Chen Z and Luo C 1998 Design and implementation of capacitive proximity sensor using microelectromechanical systems technology *IEEE Trans. Ind. Electron.* **45** 886–94
[65] Shibata T, Unno K, Makino E, Ito Y and Shimada S 2002 Characterization of sputtered ZnO thin film as sensor and actuator for diamond AFM probe *Sensors Actuators* A **102** 106–13
[66] Langer M G, Oeffner W, Wittmann H, Floesser H, Schaar H, Haeberle W, Pralle A, Ruppersberg J P and Hoerber J K H 1997 A scanning force microscope for simultaneous force and patch-clamp measurements on living cell tissues *Rev. Sci. Instrum.* **68** 2583–90
[67] Lin G, Palmer R E, Pister K S J and Roos K P 2001 Miniature heart cell force transducer system implemented in MEMS technology *IEEE Trans. Biomed. Eng.* **48** 996–1006
[68] Dargahi J, Parameswaran M and Payandeh S 2000 A micromachined piezoelectric tactile sensor for an endoscopic Grasper-theory, fabrication and experiments *J. Microelectromech. Syst.* **9** 329–35
[69] Haque M A and Saif M T A 2002 Mechanical behavior of 30–50 nm thick aluminum films under uniaxial tension *Scr. Mater.* **47** 863–7
[70] Sun Y, Nelson B J, Potasek D P and Enikov E 2002 A bulk microfabricated multi-axis capacitive cellular force sensor using transverse comb drives *J. Micromech. Microeng.* **12** 832–40